



## RESEARCH ARTICLE

10.1029/2022JG007176

### Key Points:

- Nutrients delivered by snow from marine and continental sources were supplemented by the dissolution of dust deposited from local sources
- Autotrophic communities were conspicuous by their absence within a High Arctic glacial snowpack during summer
- Secondary bacterial production therefore dominated the entire summer, with a superimposed ice layer of refrozen snowmelt providing temporary storage for low concentrations of nutrients and cells

### Supporting Information:

Supporting Information may be found in the online version of this article.

### Correspondence to:

A. Dayal,  
ard33@aber.ac.uk

### Citation:

Dayal, A., Hodson, A. J., Šabacká, M., & Smalley, A. L. (2023). Seasonal snowpack microbial ecology and biogeochemistry on a high Arctic ice cap reveals negligible autotrophic activity during spring and summer melt. *Journal of Geophysical Research: Biogeosciences*, 128, e2022JG007176. <https://doi.org/10.1029/2022JG007176>

Received 9 SEP 2022  
Accepted 30 AUG 2023


### Author Contributions:

**Conceptualization:** A. Dayal, A. J. Hodson  
**Data curation:** A. Dayal, A. L. Smalley  
**Formal analysis:** A. Dayal  
**Funding acquisition:** A. Dayal, A. J. Hodson  
**Investigation:** A. Dayal  
**Methodology:** A. Dayal, M. Šabacká, A. L. Smalley  
**Project Administration:** A. Dayal, A. J. Hodson

© 2023. The Authors.

This is an open access article under the terms of the [Creative Commons Attribution License](https://creativecommons.org/licenses/by/4.0/), which permits use, distribution and reproduction in any medium, provided the original work is properly cited.

# Seasonal Snowpack Microbial Ecology and Biogeochemistry on a High Arctic Ice Cap Reveals Negligible Autotrophic Activity During Spring and Summer Melt

A. Dayal<sup>1,2,3</sup> , A. J. Hodson<sup>2,4</sup>, M. Šabacká<sup>5</sup>, and A. L. Smalley<sup>3</sup>

<sup>1</sup>Department of Life Sciences, Aberystwyth University, Aberystwyth, UK, <sup>2</sup>Arctic Geology Department, University Centre in Svalbard, Longyearbyen, Norway, <sup>3</sup>Department of Geography, University of Sheffield, Sheffield, UK, <sup>4</sup>Department of Environmental Sciences, Western Norway University of Applied Sciences, Sogndal, Norway, <sup>5</sup>Centre for Polar Ecology, University of South Bohemia, České Budějovice, Czech Republic

**Abstract** Snowpack ecosystem studies are primarily derived from research on snow-on-soil ecosystems. Greater research attention needs to be directed to the study of glacial snow covers as most snow cover lies on glaciers and ice sheets. With rising temperatures, snowpacks are getting wetter, which can potentially give rise to biologically productive snowpacks. The present study set out to determine the linkage between the thermal evolution of a snowpack and the seasonal microbial ecology of snow. We present the first comprehensive study of the seasonal microbial activity and biogeochemistry within a melting glacial snowpack on a High Arctic ice cap, Foxfonna, in Svalbard. Nutrients from winter atmospheric bulk deposition were supplemented by dust fertilization and weathering processes.  $\text{NH}_4^+$  and  $\text{PO}_4^{3-}$  resources in the snow therefore reached their highest values during late June and early July, at 22 and 13.9  $\text{mg m}^{-2}$ , respectively. However, primary production did not respond to this nutrient resource due to an absence of autotrophs in the snowpack. The average autotrophic abundance on the ice cap throughout the melt season was  $0.5 \pm 2.7$  cells  $\text{mL}^{-1}$ . Instead, the microbial cell abundance was dominated by bacterial cells that increased from an average of  $(39 \pm 19)$  cells  $\text{mL}^{-1}$  in June to  $(363 \pm 595)$  cells  $\text{mL}^{-1}$  in early July. Thus, the total seasonal biological production on Foxfonna was estimated at 153  $\text{mg C m}^{-2}$ , and the glacial snowpack microbial ecosystem was identified as net-heterotrophic. This work presents a seasonal “album” documenting the bacterial ecology of glacial snowpacks.

**Plain Language Summary** Most research attention has been given to snow covers lying on top of soil ecosystems, and therefore we do not know enough about the ecology of glacial snowpack ecosystems. This is a major knowledge gap, given that most of the world's snow cover lies over glaciers, ice caps and ice sheets. This study shows that during the melt season on a High Arctic ice cap, Foxfonna in Svalbard, nutrients are most available during the peak of summer (June–early July transition period), but a shortage of photosynthesizing microbes can mean that they largely remain in situ until transported downstream by meltwater runoff. Processes with the capacity to generate high concentrations of essential nutrients such as N and P in snow and meltwater could therefore be described, because the primary producers did not sequester them. In contrast, an increase in bacterial cell numbers was observed during the same period. The glacial snowpack ecosystem was therefore net-heterotrophic due to the absence of autotrophs and proliferation of bacterial cells. Since the nutrient demand of the bacterial biomass is low, the ecosystem releases carbon, nitrogen, and phosphorus, rather than fixes it.

## 1. Introduction

### 1.1. The Status of Glacier Snowpack Ecosystem Research

Seasonal snowpacks cover nearly a third of the Earth's land surface at the start of summer with a mean winter maximum extent of  $47 \times 10^6$   $\text{km}^2$  (Hinkler et al., 2008). Snow covers play an integral role in the climate system via radiative feedbacks, ground insulation (Hinkler et al., 2008) and biogeochemical cycles (Wadham et al., 2013). Although snowpacks have received significant research attention, most has been in the context of snow covers lying on top of soil or other aquatic ecosystems (Jones, 1999; Kuhn, 2001; Larose et al., 2010, 2013).

What is known about glacial snowpack ecosystems is largely derived from molecular, functional, and physiological studies (e.g., Hoham & Remias, 2020; Lutz et al., 2016; Malard et al., 2019). These studies have given a great deal of attention to snow algae and glacier algae, not least due to their linkage with pigment-mediated

**Resources:** A. Dayal, A. J. Hodson  
**Software:** A. Dayal  
**Supervision:** A. J. Hodson  
**Validation:** A. Dayal  
**Visualization:** A. Dayal, A. J. Hodson  
**Writing – original draft:** A. Dayal  
**Writing – review & editing:** A. Dayal, A. J. Hodson, M. Šabacká, A. L. Smalley

albedo reduction and melt enhancement (Cook et al., 2020; Di Mauro et al., 2020; Gray et al., 2020; Williamson et al., 2019). Recently, there has been a shift from the aforementioned studies to the study of interactions between algae, fungi and bacteria (Fiołka et al., 2021; Krug et al., 2020). Although important, such approaches have not addressed fundamental ecosystem characteristics, such as links to biogeochemical processes and the changing physical conditions of a snowpack during melt. As a consequence, we are yet to understand the (re)distribution of nutrients and microbes within the different layers of a melting snowpack and how this supports the concept of the snowpack as an ecosystem, especially in the context of changing climate. From this perspective, it is expected that surface meltwater will play a critical role in the redistribution of microbes and nutrients on the surface of glaciers, including their delivery to the deeper (darker) layers of the snowpack or the glacier bed, where photosynthesis cannot occur, and heterotrophic production is likely to be dominant (e.g., Mikucki & Priscu, 2007; Skidmore et al., 2000). Additionally, one can expect the ecology of snow to be driven by the production of meltwater and the changes in the snowpack's physical condition during melt because this greatly affects the propagation of light through the snow and the transfer of nutrients by percolating liquid water (e.g., Hodson et al., 2017; Tranter & Jones, 2001). We, therefore, hypothesize that with the evolution in a snowpack's physical condition during summer melt, greater heterogeneity will be expected in microbial abundance and nutrients within the different layers of a melting snowpack (see also Nowak et al., 2018).

In addition to increased melting, the warming of the cryosphere is also changing the composition of snowpacks. For example, a surface energy/mass balance model of an Arctic glacier (Wright et al., 2007) predicted that due to rising temperatures, superimposed ice (SI) (formed following the refreezing of meltwater) will account for greater than 50% of the total accumulation by 2050. Furthermore, this SI has been shown to be a transient reservoir of nutrients/organic carbon in an earlier study on the Foxfonna ice cap (Kozioł et al., 2014, 2019). In addition, Hell et al. (2013) demonstrated that the microbial communities within the melting snowpack were structured according to habitat type, that is, most taxa showed different distributions based on the habitat (surface snow, snow, slush, and near-surface ice). This niche specificity was also demonstrated in a maritime Antarctic (Livingston Island) glacial snowpack where Hodson et al. (2017) provided evidence for differences detectable not only in the microbial community composition, but also the biomass and nutrients of coastal and inland (glacial) snowpacks, thereby highlighting changes over short distances (<1 km). A new study, carried out upon another maritime Antarctic glacier (Signy Island), also revealed such differences between two coastal sites, as well as within the vertical profile of a glacial snowpack with a substantial SI layer (Hodson et al., 2021). In this context, snowpack stratification and its effects on resident microbes and nutrients could be significant. Therefore, this study will examine whether SI forms a unique habitat or niche for microbial life.

To date, carbon balance studies in snowpacks lag behind studies in other glacial habitats, especially cryoconite holes, supraglacial streams and lakes (e.g., Cook et al., 2012; Dubnick et al., 2017). This is in spite of snowpacks being a recognized organic carbon reservoir (Priscu et al., 2008) with the ability to influence air-snow exchange processes (Amoroso et al., 2010), downstream ecosystems (Hood et al., 2015) and the carbon cycle (Wadham et al., 2019). Even fewer attempts have been made to integrate carbon into an ecosystem model that can help us understand the sources, sinks and transformations, and these have focused upon either surface glacial ice or cryoconite (e.g., Cook et al., 2012; Hodson et al., 2010a, 2010b; Stibal et al., 2017). In this study, biomass carbon will therefore be estimated, and its application to the quantification of autotrophic and heterotrophic microbial production duly considered.

We therefore present the first comprehensive study of the microbial activity and biogeochemistry of a melting snowpack on a High Arctic ice cap, Foxfonna. In so doing, we characterize seasonal changes in microbial abundance, nutrient and chlorophyll concentrations within snow, SI and glacial ice. Three main objectives were addressed:

1. To reveal the changing biogeochemistry and microbial ecology of snow throughout its evolution during the melt season.
2. To characterize the microbial and biogeochemical differences between snow, SI and glacial ice: that is, the different layers that form the habitat.
3. To establish whether this snowpack is primarily a net autotrophic or heterotrophic ecosystem.

## 2. Materials and Methods

### 2.1. Study Site

Foxfonna (78°07'–78°09'N; 16°06'–16°11'E) is a small (4 km<sup>2</sup>) mountain ice cap in Central Spitsbergen, Svalbard (Figure 1), 2.31 km in diameter with elevations mainly between 550 and 808 m.a.s.l. (Kozioł, 2014).

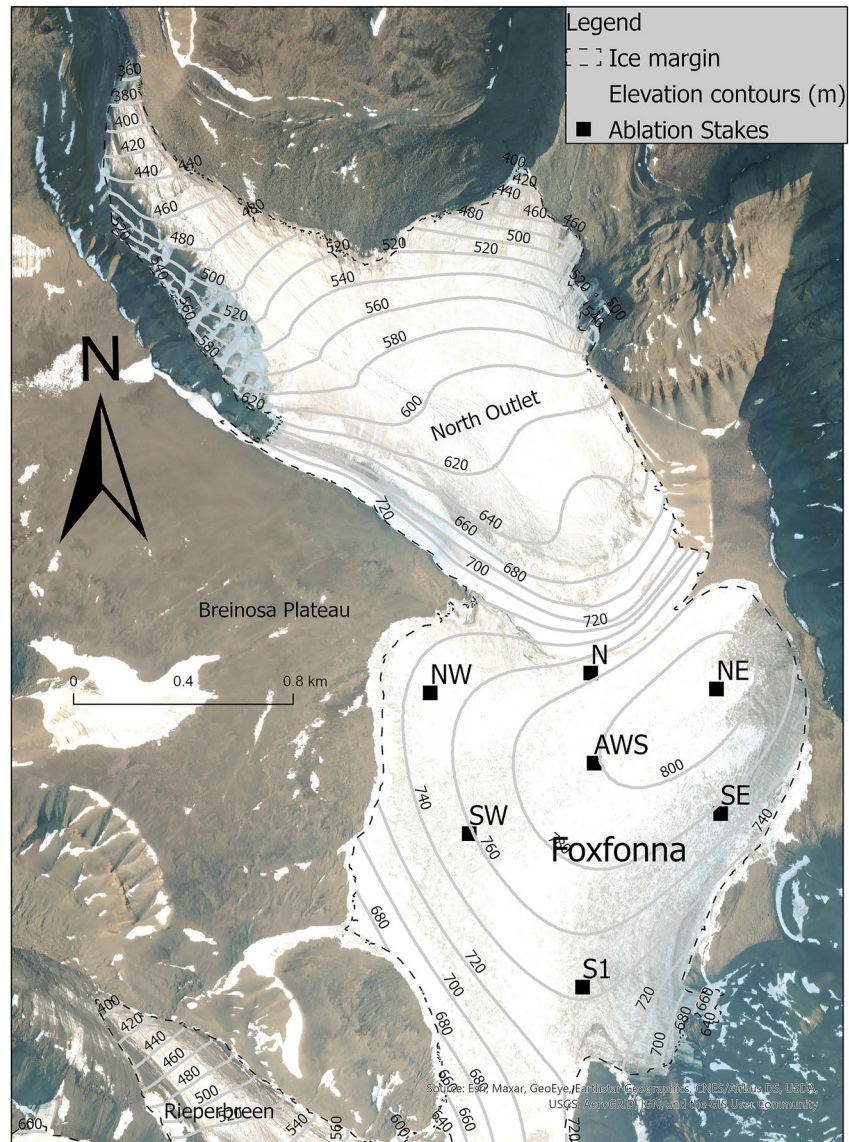


**Figure 1.** Foxfonna ice cap on Svalbard with ice margins and sampling sites marked.

Ground-penetrating radar surveys on Foxfonna show glacial ice that is less than 80 m thick (Murray, T., Unpublished Data in Rutter et al. (2011)). These surveys suggested that the ice cap is cold-based, as was established following the measurement of negative temperatures in boreholes beneath its North Outlet (Liestøl, 1993). The mass balance history of the ice cap has been observed since 2007, and to date only 2 years (2008 and 2012) have recorded net positive growth across the study site (Table S1 in Supporting Information S1). Since 2013, the annual net balance has become increasingly negative, such that the entire ice cap has become an ablation area. Perennial snow cover (firn) has been absent since the 2016 season used in the present study.

## 2.2. Snow Pit Sampling

Figure 2 presents the key changes in snow depth and thermal conditions observed during the melt season at Foxfonna, from April (pre-melt) to late July. The observation period coincided with the well-known transition seen on Svalbard glaciers that is, from a cold, low density snowpack just prior to the onset of melting, to an isothermal, ice-rich and saturated snowpack by early summer (see Wadham & Nuttall, 2002). Therefore, in April, the snowpack at Foxfonna was dry and cold with a depth of ~1.5 m at most sites. In addition, a layer of metamorphosed snow developed between the glacial ice and the overlying snowpack due to vapor and temperature



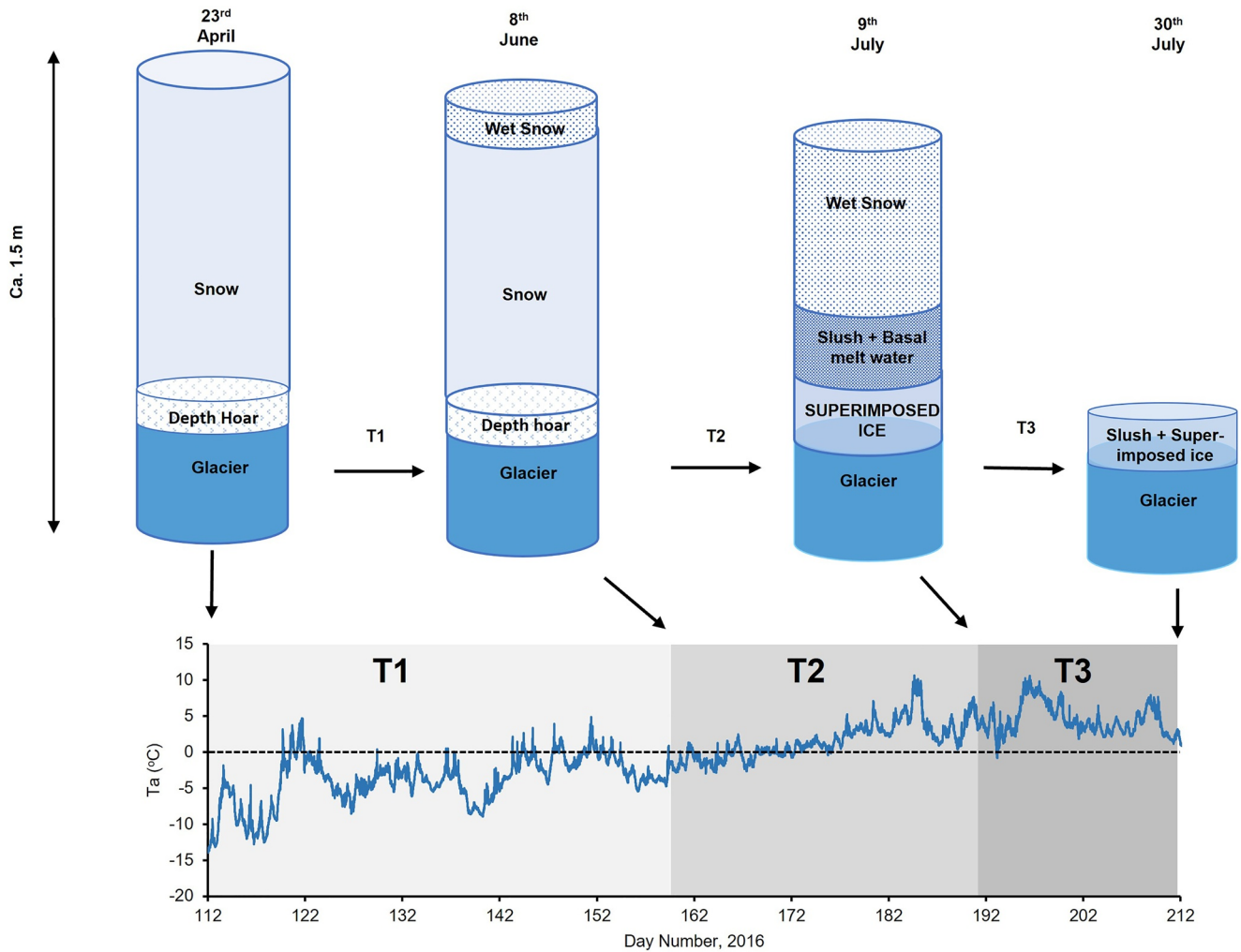


**Figure 2.** A schematic diagram showing the change in Foxfonna snowpack profile along with air temperatures (°C) observed as melt season progressed from 23 April to 30 July 2016. Transition periods marked as T1, T2, T3.

gradients during the cold period, forming a well-known depth hoar layer, that is typically less than 10 cm thick (see Möller & Möller, 2019).

A key transition period (hereafter “T1”) involved the development of a wet and larger, coarse-grained snow surface as energy became available in response to the arrival of summer (Figure 2). Although some minor melting occurred at the surface, snow temperatures remained below freezing beneath it, as evidenced by the appearance of thin ice lenses. The second important transition period, “T2,” from mid-June to early July, was marked by a sustained increase in air temperatures, which remained positive from Day Number 167 onwards (Figure 2). These conditions caused significant snowmelt and meltwater percolation toward the glacier surface, where refreezing occurred. The growth and development of SI at the snow-glacier interface during period T2 is well-known in Svalbard. It is a critical period for removing the cold content of the snowpack by latent heat release and thus producing an isothermal snowpack that lies at the melting point (see Wadham & Nuttall, 2002; Wright et al., 2007). Thereafter, isothermal melting conditions remained because no freezing air temperatures were experienced. As a consequence, the snowpack slowly melted, forming slush or ponded basal meltwater and runoff. Depletion of the snow cover then exposed the underlying layer of SI in July (transition period “T3”). Loss of this exposed SI to runoff occurred by late July. Typically, a slushy mix of larger coarse-grained snow crystals, residual SI and glacial ice was observed by this time, and glacier surface debris (cryoconite) became obvious.

Field campaigns were therefore undertaken in 2016 for the purpose of a pre-melt survey (23rd April) and to coincide with transition periods: T1 on 8th June, T2 on 9th July and T3 on 30th July (see Figure 2). Based on

the directional aspect of Foxfonna, seven stakes (NW, SW, S1, AWS, SE, NE, and N) were chosen for snow pit sampling (Figure 1). At each of the seven stakes, the following samples were collected into sterile Whirl-pak (*Nasco*) bags: surface snow (0–20 cm depth), mid snow (from 20 cm depth to the base of the snowpack), superimposed basal ice and the underlying glacier ice. These samples are hereafter referred to respectively as “TOP, MID, SUP ICE, and GL ICE.” Samples in April and June were collected using a pre-cleaned 8.5 cm diameter Federal Snow Sampling Tube (Rickly Hydrological Co.). In July, the presence of slush and thick SI required the use of a KOVACS Mark V ice corer (14 cm inner diameter) along with snow pit sampling. A consistent core length of 25 cm GL ICE was extracted at each stake (Figure 1) during the early and late July surveys only.

### 2.3. Biogeochemical Parameters

Samples stored in sterile 1L Whirl-paks (*Nasco*) were allowed to melt overnight in the dark at ambient room temperature at the University Centre in Svalbard (UNIS). Thereafter, a highly sensitive Chelsea Unilux chlorophyll fluorometer (notional detection limit of  $0.01 \mu\text{g L}^{-1}$ ) was used to provide a rapid *in vivo* chlorophyll *a* assay before cell degradation could occur. Post thaw, samples were agitated, a 10 mL aliquot immediately removed and the average of 3 fluorescence readings per sample were taken. pH measurements were conducted using a standard, portable meter and electrodes (Hanna Instruments, UK) calibrated using new pH 4 and 7 buffers. For microscopy analysis, 13 mL of subsample was removed using a sterile syringe, fixed with 1 mL of 37% formaldehyde (0.2  $\mu\text{m}$ -filtered) to get a final concentration of c. 2.5% w/v (Halbach et al., 2022) and stored in sterile 15 mL Corning centrifuge tubes. The samples for microscopy were stored in the dark at  $4^\circ\text{C}$  and analyzed within 3 months at the University of Sheffield, UK.

Analysis of other biogeochemical parameters such as nutrients and cell pigments required filtration. For nutrient analysis, 25 mL aliquots were filtered through 0.45  $\mu\text{m}$  cellulose nitrate filter paper (47 mm) using a glass filtration apparatus (acid-washed with 10% HCl). Filtered samples were stored in sterile 50 mL conical centrifuge tubes (VWR, UK). Concentrations of cations  $\text{Na}^+$ ,  $\text{K}^+$ ,  $\text{Mg}^{2+}$ ,  $\text{Ca}^{2+}$  and anions  $\text{Cl}^-$ ,  $\text{F}^-$ , and  $\text{SO}_4^{2-}$  were determined using the Dionex ICS90 ion chromatography, calibrated in the range  $0.01\text{--}1 \text{ mg L}^{-1}$  for cations and in the range  $0.25\text{--}1 \text{ mg L}^{-1}$  for anions. The precision errors for these ions ranged from 0.9% to 1.6%, while the detection limit was  $\leq 0.05 \text{ mg L}^{-1}$  (calculated as three times the standard deviation of 10 MilliQ blanks). Quantification of  $\text{NH}_4^+$ ,  $\text{PO}_4^{3-}$ ,  $\text{NO}_3^-$  and Si in the samples were conducted using a Skalar San++ Continuous Flow Analyzer, calibrated in the range  $0\text{--}3 \text{ mg L}^{-1}$ . The limit of detection for these ions was  $\leq 0.05 \text{ mg L}^{-1}$  (calculated as three times the standard deviation of 10 MilliQ blanks), while the limit of quantification was  $\leq 0.2 \text{ mg L}^{-1}$ . These analyses employed standard colorimetric methods (based on British Standards Institute, 1996, 2002, 2004, and 2005). Data for other analytes such as  $\text{Na}^+$ ,  $\text{K}^+$ ,  $\text{Mg}^{2+}$ ,  $\text{Ca}^{2+}$ ,  $\text{F}^-$ ,  $\text{SO}_4^{2-}$ , Si and Dissolved Organic Carbon (DOC) are not shown (see Tables S2–S5 in Supporting Information S1) because they are only discussed in the context of factor analysis of the entire data set (Section 3.2).

### 2.4. Pigment Concentration

Melted samples (up to 420 mL) were filtered onto 0.45  $\mu\text{m}$  Whatman glass fiber filter paper (47 mm). Filters were individually wrapped in aluminum foil and returned frozen to the UK for analysis. Further, frozen filter papers were transported insulated with reusable refrigerant polar gel packs (ThermoSafe®) in a polystyrene box to the University of Bristol and immediately stored at  $-80^\circ\text{C}$ . Filters were then freeze-dried (for 24 hr), and High-Performance Liquid Chromatography (HPLC) analysis of the samples was undertaken following procedures described in Williamson et al. (2018, 2020).

### 2.5. Epifluorescence Microscopy for Cell Counts

The glass filtration set-up was rinsed and cleaned with 70% ethanol prior to analysis and in-between samples to avoid contamination. Ten mL of sample was filtered through a 0.2  $\mu\text{m}$  Poretics Polycarbonate Track Etched Black (25 mm, *Life Sciences*) filter paper, processed, followed by the addition of a combination of SYBR Green II (*Molecular Probes*) and Propidium Iodide (PI, *Invitrogen*) stains. The stain combination comprised of 10  $\mu\text{L}$  of SYBR Green II (1x working solution) and 5  $\mu\text{L}$  of 1.5 mM PI prepared in 1 mL of Dimethyl Sulfoxide (DMSO) solution. The dual stained sample was allowed to incubate for 15 min in the dark and was then filtered. This dual-stained approach was developed from flow cytometric viability studies on freshwater and marine bacteria

(Barbesti et al., 2000; Grégori et al., 2001; Lebaron et al., 1988) as well as live/dead cell counts of bacteria in drinking water (Sysmex, Partec). The filter paper was then placed onto a glass slide, a drop of SlowFade® Diamond Antifade Mountant added to it, excess fluid removed and then covered with a coverslip, ready for imaging.

For bacterial cell counts, a Widefield Nikon Live-Cell System was used at 100x magnification, and microscopic fields were captured to count a minimum of 300 cells (Cook et al., 2020), which was not always possible (e.g., for clean snow samples). The stained samples were excited at 470 nm and detected via filter cubes. Autotrophic cell counts were undertaken at 20x, 40x, and 63x and viewed under UV (for chlorophyll *a* fluorescence) and bright-field.

After imaging, images were converted to 8-bit greyscale on the software ImageJ. Cells were counted using the *Analyze Particles* function with a size range of 0.2–2  $\mu\text{m}^2$  and a circularity of 0–1. This was done to exclude the counting of mineral debris and remove noise. Filamentous bacteria or snow algae were measured manually on the software, as they were larger (10–20  $\mu\text{m}$ ). The cell counts (cells  $\text{mL}^{-1}$ ) were calculated as a product of the counts per image and the microscope's field of view, divided by the volume of the sample filtered.

### 3. Results

#### 3.1. Seasonal Change in Snow Cover, Nutrients, Cells and Chlorophyll on Foxfonna

The glacier mass balance conditions that were experienced during the study included the joint highest (i.e., 54 cm w.e.) winter snow accumulation since records began in 2007. The summer ablation was the fourth highest for the same interval (average 119 cm w.e.), causing a near-complete disappearance of the snowpack during the summer that is rather typical of this site. Figure 3a shows the evolution of the average snow water equivalent (SWE) through the melt season. Average values for the seven stakes ranged from 53 to 56 cm water equivalent (w.e.) from April until early July, and then dropped to 8 cm w.e. by the end of July (including any residual SI): most of which was near Stake N. Growth of SI commenced during T2 (June–early July) and formed an average water equivalent of  $11 \pm 5.4$  cm w.e. (not shown). Depletion of combined snow and SI to  $1 \pm 2.5$  cm w.e. occurred during transition period T3 (early–late July), according to the late July survey. In late July, the high standard deviation was due to SI being left at only one stake (AWS).

Nutrient loading at each stake was calculated from the product of the SWE (cm–w.e.) of separate TOP, MID, and SUP ICE samples and their corresponding nutrient concentration ( $\text{mg L}^{-1}$ ), which were then summed to produce the total mass (or “loading”) at each stake location in  $\text{mg m}^{-2}$  (Equation 1). The coefficient 10 accounts for units of *C* being  $\text{mg L}^{-1}$  instead of  $\text{mg m}^{-3}$ , and units of SWE being cm w.e. instead of m w.e.

$$\text{Loading} = 10 \sum_{\text{TOP,MID,SI}} [\text{SWE} \times C] \quad (1)$$

Averages of the loading values at the stakes were then estimated for each survey to reveal seasonal changes across the entire ice cap. Comparison between SWE and  $\text{Cl}^{-}$  loadings (Figures 3a and 3b) show leaching of  $\text{Cl}^{-}$  from the snowpack between June and early July (i.e., transition period T2), because the  $\text{Cl}^{-}$  loading decreased more rapidly than SWE. Average  $\text{Cl}^{-}$  loadings for the entire ice cap stayed below  $1,000 \text{ mg m}^{-2}$  with the lowest value observed at the end of July:  $53 \pm 85 \text{ mg m}^{-2}$ . By comparison, loadings of  $\text{NH}_4^{+}$  and  $\text{PO}_4^{3-}$  were as much as two orders of magnitude lower, as is expected in such an oligotrophic environment.  $\text{NH}_4^{+}$  ranged from 1 to  $22 \text{ mg m}^{-2}$  and  $\text{PO}_4^{3-}$  ranged even lower, at 0.4–13.9  $\text{mg m}^{-2}$  through the melt season. Interestingly, during T2 (June–early July),  $\text{NH}_4^{+}$  and  $\text{PO}_4^{3-}$  loadings increased whilst  $\text{Cl}^{-}$  and  $\text{NO}_3^{-}$  decreased. In fact,  $\text{NH}_4^{+}$  and  $\text{PO}_4^{3-}$  loadings reached their highest values sometime after the onset of significant melting during early July at 22 and  $13.9 \text{ mg m}^{-2}$  respectively. Surprisingly,  $\text{NO}_3^{-}$  did not show its highest loading at the same time as  $\text{NH}_4^{+}$ . Instead,  $\text{NO}_3^{-}$  was leached rather like  $\text{Cl}^{-}$  and ranged from 0.5 to  $15.4 \text{ mg m}^{-2}$ .

Bacterial cell loading (cells  $\text{m}^{-2}$ ) at each stake was calculated in an identical manner to the nutrient loading estimates (Figure 3f). Seasonal variations in the average cell loading across Foxfonna revealed minimal change during transition period T1. In contrast, an increase in cells  $\text{m}^{-2}$  occurred during transition period T2 (June–early July) from  $5.3 \times 10^6 (\pm 2.7 \times 10^5)$  to  $3.8 \times 10^7 (\pm 4.3 \times 10^6)$  where *p*-value = 0.05 and  $\alpha = 0.05$ . A decrease to  $6.1 \times 10^6 (\pm 1.6 \times 10^6)$  cells  $\text{m}^{-2}$  followed during T3 (early to late July), although this was insignificant at the 95% confidence level (*p*-value = 0.3 where  $\alpha = 0.05$ ), due to strong spatial variability in cell concentrations.

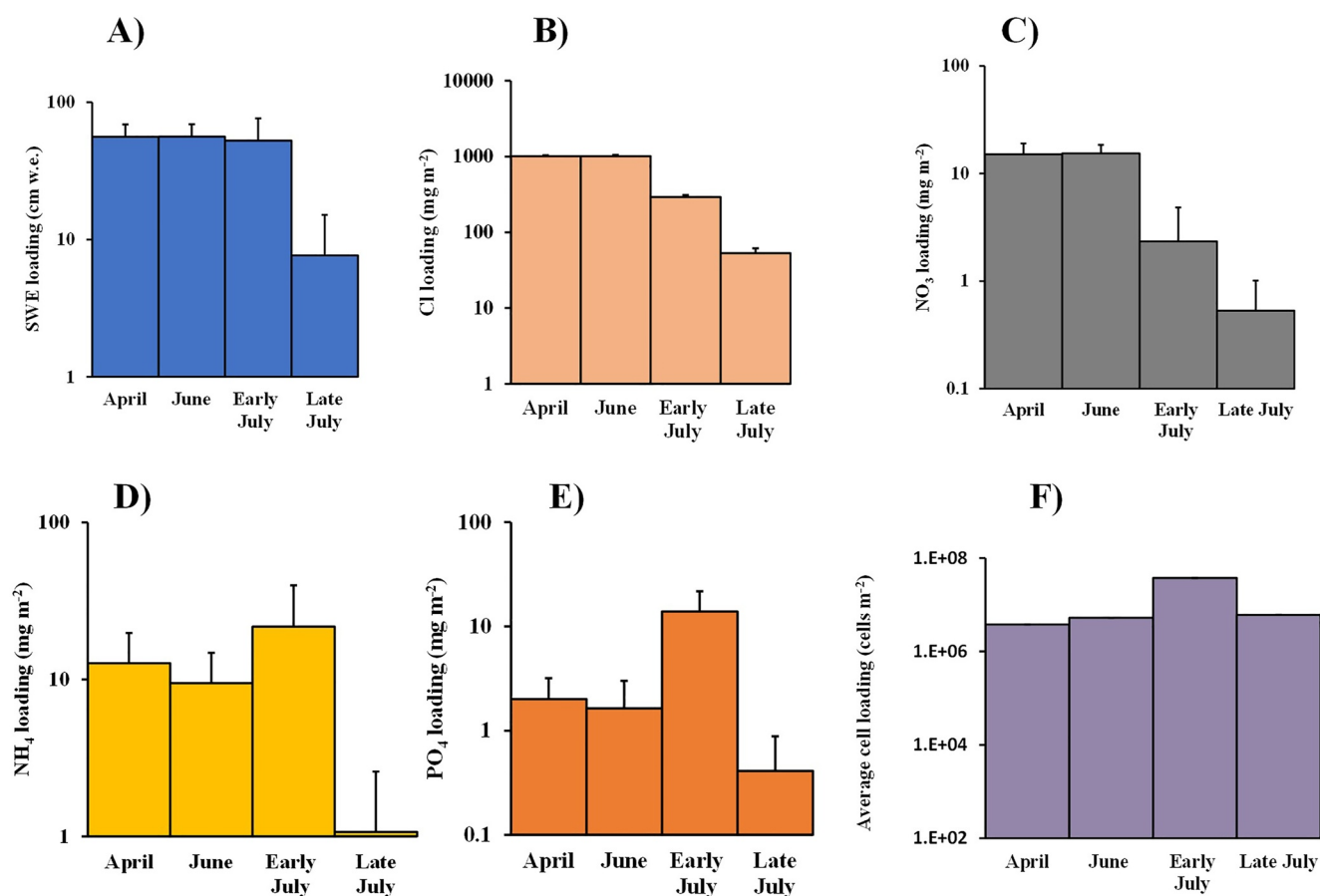


**Figure 3.** Seasonal change in snow water equivalent, average loadings ( $\text{mg m}^{-2}$ ) for  $\text{Cl}^-$ ,  $\text{NO}_3^-$ ,  $\text{NH}_4^+$ ,  $\text{PO}_4^{3-}$  and cell loading on Foxfonna ice cap. Error bars are standard deviations ( $n = 7$ ).

Chlorophyll *a* was the dominant pigment within snow, SI and glacial ice (Figure S2 in Supporting Information S1). The Unilux derived chlorophyll *a* concentration within snow, SI and glacier ice ranged between 1.7 and 13  $\mu\text{g L}^{-1}$  (Figure S3 in Supporting Information S1). There was no significant change within the TOP and MID snows during transition periods T1 and T2, that is, between April and June, where it lay in the range 1.7–2.7  $\mu\text{g L}^{-1}$  and from June to early July, 1.7–1.9  $\mu\text{g L}^{-1}$ . GL ICE displayed the highest chlorophyll *a* concentration at 13 and 10.7  $\mu\text{g L}^{-1}$  in early and late July, respectively. However, when the snow samples were examined under the microscope, no autotrophic cells were detected in most samples. Therefore, a comparison between the Unilux-measured (in vivo fluorescence) chlorophyll *a* and HPLC-derived extracted chlorophyll *a* concentrations was undertaken using bulk samples. This yielded a moderate correlation ( $r = 0.77$ ,  $p < 0.05$ ) with a significant intercept of 2.1  $\mu\text{g L}^{-1}$ , indicating the presence of a non-biological signal affecting the Unilux sensor (Figure S4 in Supporting Information S1). Furthermore, the “background” Unilux measurements for samples with no detectable autotrophs (according to microscopy) was almost always 2  $\mu\text{g L}^{-1}$ . Therefore, it is highly likely that another source of fluorescence—such as mineral autofluorescence—is present in the signal, and so the Unilux readings cannot be used to reliably detect the presence of autotrophs in low numbers.

### 3.2. Factor Analysis

Factor analysis was undertaken to establish the sources and differential behavior of the nutrients, cells and chlorophyll. All major ions, DOC and Si were included in the analyses. To preserve the variance in the entire data set, all the separate TOP, MID and SUP ICE samples were used, rather than combined values for each stake. The statistical package Statistical Package for the Social Sciences identified six factors with Eigen Values  $> 1$ , which collectively explained 76% of the total variance in the data set. However, only the first three factors produced strong

**Table 1**  
Factor Loading Analysis for All Samples Through the Melt Season

Parameter	Factor 1	Factor 2	Factor 3
Na <sup>+</sup>	0.794**	-0.090	0.074
K <sup>+</sup>	0.004	-0.113	0.758**
Mg <sup>2+</sup>	0.778**	0.265	0.158
Ca <sup>2+</sup>	0.688**	0.496*	0.228
F <sup>-</sup>	0.293	0.081	-0.041
Cl <sup>-</sup>	0.769**	-0.286	0.189
NO <sub>3</sub> <sup>-</sup>	0.610**	-0.473*	-0.211
NH <sub>4</sub>	-0.268	-0.277	0.727**
PO <sub>4</sub> <sup>3-</sup>	-0.743**	0.111	0.354
SO <sub>4</sub> <sup>2-</sup>	0.650**	-0.205	-0.108
Si	-0.648**	0.012	0.254
Chlorophyll <i>a</i> (Chl)	0.235	0.695**	0.320
Autotrophic cell abundance	0.094	0.213	-0.165
Total cell abundance	-0.200	0.718**	-0.277
Dissolved Organic Carbon (DOC)	0.433*	0.606**	0.403*

Note. Moderate loadings (i.e., between 0.4 and 0.69) and strong loadings (i.e., >0.7) are marked by “\*” and “\*\*” respectively.

loadings (>0.7) and were thus amenable to interpretation. Table 1 shows these three factors, highlighting the variables with either strong or moderate loadings (between 0.4 and 0.69) in each case. The first Factor (F1) showed strong positive loadings in the order Na<sup>+</sup>, Mg<sup>2+</sup>, Cl<sup>-</sup>, Ca<sup>2+</sup>, SO<sub>4</sub><sup>2-</sup>, and NO<sub>3</sub><sup>-</sup>. There were also strong or moderate negative loadings from PO<sub>4</sub><sup>3-</sup> and Si. At first glance, Factor 1 seems to be dominated by marine aerosol. However, ratios of Ca<sup>2+</sup> to Cl<sup>-</sup> (both being strong contributors to Factor 1) were in excess of standard marine water ratios, showing a significant non-sea-salt supply of Ca<sup>2+</sup> (average 85%; data not shown). Therefore, Factor 1 most likely reflects the leaching (elution) of solute from the snowpack, which is dominated by (but is not exclusive to) solute derived from marine aerosol. The strong or moderate negative loadings of PO<sub>4</sub><sup>3-</sup> and Si respectively were unexpected, but might indicate a different source that became more apparent as the elution of mobile ions progressed.

The second Factor (F2) explained 16% of the variance in the data set, and was dominated by moderate to strong loadings for DOC, total cell abundance (i.e., the sum of bacterial and autotrophic cells) and chlorophyll *a* (0.61, 0.72, and 0.69). It is tempting to suggest that photosynthetic microbes such as cyanobacteria might be responsible for the presence of all three of these variables, but no significant loading was observed with the autotrophic cell abundance due to their absence in the snow. Instead, it seems more likely that Factor 2 represents similar behavior of bacterial cells, DOC and small, auto-fluorescent mineral particles that perhaps cause variations in the background chlorophyll *a* readings. Therefore Factor 2 most likely reflects the mobility of particles in the snow matrix during the summer and their provision of NH<sub>4</sub><sup>+</sup>.

Like Ca<sup>2+</sup>, K<sup>+</sup> showed a strong non-marine contribution (average 91%), yet it loaded strongly onto F3 along with NH<sub>4</sub><sup>+</sup> (0.76 and 0.73, respectively). This is most likely indicative of dust or clay weathering processes, as NH<sub>4</sub><sup>+</sup> and K<sup>+</sup> act as interchangeable cations in clay-mineral lattices, and are easily extractable following adsorption onto dust or clay particles.

### 3.3. Seasonal Bacterial Production on Foxfonna

Bacterial cell loading estimates (Figure 3f) were used to estimate the total bacterial biomass on Foxfonna, such that the bacterial production (BP) could be estimated from rate of change in biomass (BM) per unit time (Takacs & Priscu, 1998). Bacterial production was assumed to be negligible during period T1 on account of there being very little liquid water in the cold snowpack (see Figure 2). Therefore, period T2 was the most suitable period for applying this approach, because changes in cell loading were likely dominated by BP on account of the high-water content and its capillary retention within the snow (Reijmer et al., 2012). The loss or gain of bacterial cells by wind-blown snow transport is also likely to have been suppressed greatly by the high-water content in the older snow, and the lack of fresh snowfall events (hence the negligible change in total SWE during T2 on the ice cap shown in Figure 3a).

Under the assumption that only bacterial growth dominated the bacterial cell loading change during transition period T2, BP in snow and superimposed was estimated thus:

$$BP_{\text{snow}\pm\text{SI}}^{\text{T2}} = c \cdot \left( \frac{\overline{BM}_{\text{snow}}^{\text{early july}} - \overline{BM}_{\text{snow}}^{\text{june}} + \overline{BM}_{\text{SI}}^{\text{early july}}}{T2} \right) \quad (2)$$

Where  $BP_{\text{snow}\pm\text{SI}}^{\text{T2}}$  is the combined average daily BP during T2 for snow and SI (mg C m<sup>-2</sup> d<sup>-1</sup>), T2 is the transition period duration that is, 32 days, BM is average biomass, estimated from average snow or SI cell loading on the ice cap (cells m<sup>-2</sup>). Note that since no SI layer existed in June, only its cell content in the early July survey needed to be included in the census. Finally,  $c$  = carbon content of each cell according to Takacs and Priscu (1998).

The results suggest transition period T2 was marked by an increase in bacterial biomass by an order of magnitude throughout the entire snow/ice layer of  $2.4 \pm 1.5 \times 10^{-5}$  mg C m<sup>-2</sup> d<sup>-1</sup>. Of this, up to  $1.0 \pm 0.5 \times 10^{-5}$  mg C



**Table 2**  
Average Cell Abundance on Foxfonna

Sample type	Month	Snow algae (cells mL <sup>-1</sup> )	Cyanobacteria (cells mL <sup>-1</sup> )	Bacteria (cells mL <sup>-1</sup> )
All Snow	April	0	5 ± 9	81 ± 124
	June	0	0	39 ± 19
	Early July	0.2 ± 0.4	0	363 ± 595
	Late July	0.1 ± 0.3	0.7 ± 1.5	935 ± 1,460
SUP ICE	Early July	0.04 ± 0.1	0	299 ± 306
	Late July	0.3 ± 0.5	0.1 ± 0.4	185 ± 0
GL ICE	Early July	0.5 ± 0.7	0.1 ± 0.4	565 ± 575
	Late July	0.3 ± 0.6	2 ± 4	818 ± 792

Note. Values are average ± standard deviation.

m<sup>-2</sup> d<sup>-1</sup> was stored in SUP ICE. Biological production cannot be separated between snow and SI, because all of the bacteria in the ice could have been washed downwards whilst the SI was forming.

Although conditions were similar during T3, this transition period was dominated by runoff, as shown by the marked SWE depletion in Figure 2. Therefore, it is important to take into account the loss of cells with this runoff, as indicated below. However, it must be noted that cells lost during runoff are more likely to be bacterial than autotrophic, because they are smaller and the autotrophic cells have a propensity to form cryoconite aggregates and persist for several years on the glacial surface (Hodson et al., 2010a, 2010b).

$$BP_{\text{snow}\pm\text{SI}}^{\text{T3}} = c \cdot \left( \frac{\overline{BM}_{\text{snow}}^{\text{late july}} - \overline{BM}_{\text{snow}}^{\text{early july}} + \overline{BM}_{\text{SI}}^{\text{late july}} - \overline{BM}_{\text{SI}}^{\text{early july}} + RU_{\text{cells}}^{\text{T3}}}{T3} \right) \quad (3)$$

where  $RU_{\text{cells}}^{\text{T3}}$  is the runoff flux of cells normalized for ice cap area (i.e., cells m<sup>-2</sup>) and T3 is the duration of Transition period 3, that is, 23 days.

However, uncertainty in  $RU_{\text{cells}}$  is such that biological production could not be estimated directly during this period. Daily rates of BP in the snowpack and the SI during T3 were therefore assumed to be half of that deduced from T2, to account for the depletion of SWE to almost zero during this interval.

The rates of seasonal BP were therefore estimated to be negligible in transition period T1 (due to low free water content within the snow), to be  $2.4 \pm 1.5 \times 10^{-5}$  mg C m<sup>-2</sup> d<sup>-1</sup> during transition period T2 and to be  $1.2 \pm 0.75$  mg C m<sup>-2</sup> d<sup>-1</sup> during transition period T3. The near-complete ablation of the snowpack and SI after this means their contribution to BP would have been negligible, and the ecosystem dominated by biological production upon the glacier surface. The total BP within the snow and SI for the combined 55 days of T2 and T3 was therefore 153 mg C m<sup>-2</sup> a<sup>-1</sup>.

### 3.4. Spatial Variations in Nutrient Concentrations and Cells

“TOP” and “MID” snow samples were compared with the SI and glacial ice samples (“SUP ICE” and “GL ICE,” respectively) with respect to the essential macronutrients NH<sub>4</sub><sup>+</sup> and PO<sub>4</sub><sup>3-</sup>, due to the unexpected increase in their concentrations revealed by Figures 3d and 3e. We found that average NH<sub>4</sub><sup>+</sup> concentrations ranged from 0 to 0.04 mg L<sup>-1</sup> in the April samples of TOP and MID snow (Figure S1 in Supporting Information S1). However, after the onset of melt and SI formation, greater average NH<sub>4</sub><sup>+</sup> concentrations (0.05 ± 0.05 mg L<sup>-1</sup>) appeared in SUP ICE than in the TOP and MID snows (0.03 ± 0.01 and 0.04 ± 0.03 mg L<sup>-1</sup>, respectively). Concentrations in GL ICE were higher still, but more variable (average 0.07 ± 0.1 mg L<sup>-1</sup> in early July). The variability was caused by high values at Stake SE (Data Not Shown): a site notable for a high concentration of surface debris. Average PO<sub>4</sub><sup>3-</sup> concentrations were an order of magnitude lower than NH<sub>4</sub><sup>+</sup> in April and June that is, between 0.003 and 0.005 mg L<sup>-1</sup> in TOP and MID snows (Figure S1 in Supporting Information S1). No PO<sub>4</sub><sup>3-</sup> was detected in the top layer at stake S1. However, these concentrations increased in early July and ranged from 0.02 to 0.03 mg L<sup>-1</sup> in TOP and MID snows. SUP ICE exhibited similar concentrations (average 0.03 ± 0.007 mg L<sup>-1</sup>).

Table 2 shows autotrophic (snow algae and cyanobacteria) and bacterial concentrations (in cells mL<sup>-1</sup>). Average cells mL<sup>-1</sup> are given for all snow (TOP and MID combined), SUP ICE and GL ICE. The average autotrophic cell abundance on the ice cap through the melt season was  $0.5 \pm 2.7$  cells mL<sup>-1</sup>. The large standard deviation throughout the data set indicates high spatial variability. All the autotrophic cells in April snow were identified as cyanobacteria, of which 68% were found on the southern and uppermost part of the ice cap (Stakes S1, SW, and AWS). Surprisingly, no significant numbers of autotrophic cells were identified in snow for June, early July or late July. No significant numbers of autotrophic cells were observed in SI either. The only changes in average autotrophic cell abundance were identified from early to late July due to increases in cyanobacteria (e.g.,  $0.1 \pm 0.4$ – $2 \pm 4$  cells mL<sup>-1</sup> in GL ICE) and also snow algae (e.g.,  $0.04 \pm 0.1$ – $0.3 \pm 0.5$  cells mL<sup>-1</sup> in SUP ICE). However, snow algal cells were so few and dispersed that their average number on the ice cap often resulted in an unusable value (~0 cells mL<sup>-1</sup>). By contrast, the average bacterial abundance on the ice cap was far greater and increased by an order of magnitude from ca. 10<sup>2</sup> cell mL<sup>-1</sup> to almost 10<sup>3</sup> cells mL<sup>-1</sup>. Table 2 shows that changes

in the bacterial cell abundance of SUP ICE and GL ICE were more muted than changes in the total snowpack bacterial cell abundance. It also shows that both bacteria and autotrophic cell abundance decreased between April and June. However, the decrease is an artifact of two highly concentrated samples at Stake N that were encountered in April (data not shown). Spatial variability is therefore a major characteristic of the cell distribution across the ice cap, and we could discern no clear patterns underlying this variability, either from stake to stake, or amongst the different sample types.

## 4. Discussion

### 4.1. Nutrient Sources and Their Non-Conservative Behavior in the Snowpack

Despite being largely associated with long-range atmospheric pollution (Kühnel et al., 2013),  $\text{NO}_3^-$  showed a strong, positive loading onto Factor 1 that was similar to that of  $\text{Cl}^-$ , a biogeochemically conservative ion associated with marine aerosol. Therefore,  $\text{NO}_3^-$  co-eluted with  $\text{Cl}^-$  and seems to have been largely conservative during meltwater export (e.g., Tranter & Jones, 2001). By contrast, Figure 3 shows that,  $\text{NH}_4^+$  and  $\text{PO}_4^{3-}$  demonstrated a marked increase in abundance during July, resulting in either a negative loading onto Factor 1 ( $\text{PO}_4^{3-}$ ) or loading onto the separate Factor 3 ( $\text{NH}_4^+$ ). Thereafter, both  $\text{NH}_4^+$  and  $\text{PO}_4^{3-}$  demonstrated an equally marked decrease during July (period T3), which seems to be caused entirely by the rapid ablation of the snowpack. Since the initial, sharp increase in  $\text{NH}_4^+$  and  $\text{PO}_4^{3-}$  coincided with period T2, when liquid water availability rose markedly within the snow matrix, we invoke a dissolution process involving wind-deposited clay and dust particles as the cause.

Dust deposition onto Foxfonna is well known due to the exposure of the desiccated Adventdalen river bed prior to early summer inundation by meltwater (as well as afterward in early winter). Therefore, it is likely local dust deposited at the surface (early summer) and the base (early winter) of the 2015/2016 snowpack was available for dissolution. Interestingly, the apparent conservative behavior of  $\text{NO}_3^-$  during the same period provided no evidence for oxidation of the  $\text{NH}_4^+$  to  $\text{NO}_3^-$ , as has been proposed in dry winter snowpacks by Amoroso et al. (2010). However, conversion of  $\text{NH}_4^+$  to  $\text{NO}_3^-$  is readily observed when snowmelt passes through environments that offer greater rock-water contact than the snowpack, such as those at the margins of glaciers (e.g., Hodson et al., 2010a, 2010b).  $\text{NO}_3^-$  therefore seems to be largely governed by elution when residence times are reduced by the onset of melting during summer.

In summary, local dust-derived sources of  $\text{NH}_4^+$  and  $\text{PO}_4^{3-}$  appear to have combined with long range (marine and anthropogenic aerosol) sources responsible for  $\text{NO}_3^-$  to deliver critical macro-nutrients to the Foxfonna snowpack during 2015/2016.

### 4.2. No Utilization of Nutrients by Autotrophic Communities

The present study demonstrated nutrient behavior not shown by biologically active snowpacks elsewhere, because the  $\text{NH}_4^+$  and  $\text{PO}_4^{3-}$  released by weathering processes during T2 were not sequestered for autotrophic growth and activity. The acquisition of macronutrients such as  $\text{NH}_4^+$ ,  $\text{NO}_3^-$ , and  $\text{PO}_4^{3-}$  from rock debris and marine fauna in Antarctica is well known to stimulate autotrophic growth in nutrient-limited snowpacks (Fujii et al., 2010; Hodson et al., 2017). For example, in coastal snowpacks of Livingston Island, Antarctica, the removal of  $\text{NH}_4^+$  and  $\text{PO}_4^{3-}$  from the snow correlated with increasing chlorophyll *a* concentrations that were significantly greater than those reported at Foxfonna. Therefore utilization of these nutrients by the resident autotrophic communities was a dominant feature of the Livingston Island data set (Hodson et al., 2017). Similar, order of magnitude changes in chlorophyll *a* concentrations were also observed in nutrient-enriched glacial snowpacks of Signy Island in the maritime Antarctic (Hodson et al., 2021). Here, flow cytometry analysis revealed a high autotrophic abundance (nearly  $10^5$  cells  $\text{mL}^{-1}$ ) at a chlorophyll *a* concentration of  $\sim 1 \mu\text{g L}^{-1}$ . However, enumeration by microscopy was not undertaken in either of these studies, making further comparison difficult. In spite of this, the uptake of available nutrients, resulting in an increase in the chlorophyll *a* content of the snowpack seems conspicuous by its absence at Foxfonna, and so an explanation is sought below.

Nutrients that have yet to be considered could have been responsible for limiting algal growth, such as dissolved inorganic carbon or Fe (Hamilton & Havig, 2017). However, the local geology of Adventdalen valley is dominated by sandstones, siltstones and shales (Rutter et al., 2011), whose dust is likely to yield both DIC and Fe following deposition onto the snow (e.g., Harrold et al., 2018). Their acquisition from a range of natural weathering

processes is described in the geochemical analysis of pore waters from a 4 m thick sequence of aeolian deposits immediately north of Foxfonna (Jones et al., 2020). Therefore, nutrient limitation seems to be an unlikely explanation for the lack of autotrophic growth on Foxfonna during the study period. Furthermore, a recent study did encounter a significant population of red snow algae and ice algae in snow and ice samples on Foxfonna (Fiolka et al., 2021). This study was conducted in late August in 2011, and suggests, in accordance with the authors' own observations throughout 16 years of mass balance survey, that there is marked annual variability in snow algae population dynamics.

An important environmental factor is likely to have been the role that the vertical heterogeneity of the snowpack plays in governing how conducive it becomes for autotroph proliferation, especially since a great many microorganisms would be expected to reside on the glacier surface prior to the onset of snowmelt (Stibal et al., 2015). For example, the nutrient resource available within the snowpack layers (Figure 3) would have presented an excellent opportunity for flagellated vegetative forms of green algal cells to make their way upwards toward the snow surface, seeking light and nutrients (Stibal et al., 2007). However, their motility from the glacier surface through the snowpack was most likely impeded by the refrozen SI layer and other ice lenses that formed during transition period T2.

Given the above, the most important limitation to the autotrophic production was probably insufficient inocula of snow algal cells within the fresh winter snowpack (and potentially upon the previous summer surface) to allow germination of new cells (Hoham et al., 2006). We propose that the negligible autotrophic cell abundance was also caused by the onset of sustained negative mass balance of Foxfonna from 2013 onwards. Since 2012, there have been no net positive accumulation years at the site and summer mass losses have increased markedly, resulting in the complete depletion of the firn layer and large meltwater runoff fluxes from all over the ice cap. Collectively, these most likely removed both the available inocula and the habitat required for its survival in the years preceding the present study. Furthermore, the community typically has only a short opportunity to respond to the increase in energy and nutrients during summer (55 days) before biomass is removed by further ablation (e.g., Onuma et al., 2022). Following such heavy melt years, bringing new inocula to the relatively high altitude of the ice cap at Foxfonna probably requires the wind-borne delivery of new snow algae from soils (Kvídárová, 2012), because they are more susceptible to wind erosion than snow in the summer. For example, the snow algae communities that inhabit high altitude penitente ice at 5,277 m asl (Vimercati et al., 2019) are primarily inoculated by wind-borne tephra soils, which provide a suitable habitat for part of the snow algae life cycle (Remias et al., 2012). At Foxfonna, it seems that the principal dust sources are less capable of delivering viable cells than they are nutrients. Finally, since the environment under study is by no means unique, the likely response of the snowpack autotrophic community in other high elevation polar ice caps subject to increasingly negative mass balances might also be restricted in this way, suggesting that many will be dominated by BP as they lose their perennial firn layers.

### 4.3. Assessing the Importance of Bacterial Carbon Production on Foxfonna

Significant changes in carbon resources were detectable during T2 because bacterial cell abundance increased from  $39 \pm 19$  to  $363 \pm 595$  cells  $\text{mL}^{-1}$  (Table 2). These bacterial cell numbers are more representative of Antarctic snows (Carpenter et al., 2000; Michaud et al., 2014) than the Arctic or Alpine snows (Amato et al., 2007) and were used to estimate BP during transition periods T2 and T3 at ca.  $153 \text{ mg C m}^{-2} \text{ a}^{-1}$  (Section 3.2). For these calculations, a fixed bacterial carbon content per cell ( $11 \text{ fg C cell}^{-1}$ ) was employed based on prior work on carbon reservoirs in polar habitats (Kepner et al., 1998; Priscu et al., 2008; Takacs & Priscu, 1998). This value of  $11 \text{ fg C cell}^{-1}$  had been previously used: (a) to calculate carbon released from microbial populations via viral lysis in Antarctic lakes (Kepner et al., 1998), (b) to understand the bacterioplankton dynamics in permanently ice-covered lakes in the McMurdo Dry Valleys, Antarctica (Takacs & Priscu, 1998), and most importantly, (c) to estimate prokaryotic cellular carbon reservoir in all Antarctic habitats, namely, lakes, subglacial aquifers and the ice sheets (Priscu et al., 2008). These estimates, although published in 2008, did not use any of the available allometric and linear volume-to-carbon conversion factors. These factors, compiled by Posch et al. (2001), were, however used by Bellas et al. (2013) to estimate a range for bacterial carbon production in Arctic cryoconite sediments.

Irvine-Fynn et al. (2012) quantified cell budgets on an Arctic glacier surface using flow cytometry, compared both cell-to-carbon and volume-to-carbon conversions, but opted for the higher value of  $20 \text{ fg C cell}^{-1}$  from

**Table 3**  
*Cell-To-Carbon and Volume-To-Carbon Bacterial Carbon Production Values During T2 (June–Early July) on Foxfonna*

Sampling survey (transition period)	Estimated areal bacterial production (mg C m <sup>-2</sup> day <sup>-1</sup> ) in snow
Cell-to-carbon	* $2.4 \times 10^{-5} \pm 4 \times 10^{-5}$ <sup>†</sup> $4.3 \times 10^{-5} \pm 7.3 \times 10^{-5}$
Allometric C-per-cell	<sup>~</sup> $1.2 \pm 2$ <sup>†</sup> $1.9 \pm 3.2$

*Note.* Cellular carbon content \*11 fg C cell<sup>-1</sup> (Takacs & Priscu, 1998), <sup>†</sup>20 fg C cell<sup>-1</sup> (Whitman et al., 1998), <sup>~</sup>assumes allometric C-per-cell from <sup>\*</sup>Felip et al. (2007) and <sup>†</sup>Posch et al. (2001).

Whitman et al. (1998), to estimate annual carbon export from a supraglacial catchment on Midtre Lovénbreen (Svalbard). In their study, the cell abundance, size and shape were enumerated through flow cytometry, classified on the basis of size. With the greatest proportion of cells being  $\leq 3 \mu\text{m}$ , they were presumed to be spherical-shaped heterotrophic bacteria. It is also interesting to note that the value of 20 fg C cell<sup>-1</sup> applied for heterotrophic cell carbon production by these authors, has also been used to estimate autotrophic snow algal carbon production in several Arctic/Antarctic carbon estimation studies (e.g., Fogg, 1967; Takeuchi et al., 2006). On the other hand, for their allometric volume-to-carbon estimation, wherein spherical shaped cells were assumed, the formula given by Felip et al. (2007) was applied:

$$CC = 120 \times V^{0.72} \quad (4)$$

where CC is the carbon content (fg C cell<sup>-1</sup>) and V is the biovolume ( $\mu\text{m}^3$ ).

This formula, however, was used for rod-shaped bacteria to study bacterial biomass in mountain lakes (Felip et al., 2007), and earlier to estimate biomass in the snow and ice covers of such lakes (Felip et al., 1995). This allometric model was originally given by Norland et al. (1993), where the geometric shape of the bacteria was approximated as a cylinder with hemispherical ends, based on electron microscopy and X-ray analysis of bacterial cultures. It is unclear whether the carbon content formula stays relevant for spherical bacterial cells or was intended to be used only for rod-shaped cells. This shows that differences in methods for volume estimation and the carbon content, can introduce significant variability in the carbon budget estimations and therefore the need arises to have a consensus and a standard on the parameters that are to be used for such estimations.

The summary of conversion factors from Posch et al. (2001) incorporates different size range, habitat, preparation techniques and growth conditions, but would have benefited from inclusion of a column listing the method for volume estimation involved in each of the referenced methods. Therefore, the worker needs to be careful and take into account the different parameters being used during selection of the appropriate model for their use. It might not be possible to reach a worldwide consensus on carbon estimation protocols yet, but it is important that a laboratory group produce repeatable estimations following a standard protocol so that they may be comparable and significant errors can be avoided.

For comparison purposes, Table 3 compiles bacterial carbon production numbers on a daily basis for all cell-to-carbon and volume-to-carbon conversions calculations discussed above. For obvious reasons, using 20 fg C cell<sup>-1</sup> instead of 11 fg C cell<sup>-1</sup> results in a bacterial carbon production value which is nearly double (e.g., for snow:  $2.4 \times 10^{-5} \pm 4 \times 10^{-5}$  and  $4.3 \times 10^{-5} \pm 7.3 \times 10^{-5}$  mg C m<sup>-2</sup> day<sup>-1</sup>). In contrast, the cell-to-volume allometric conversions are  $\sim 5$  orders of magnitude higher ( $1.2 \pm 2$  and  $1.9 \pm 3.2$  mg C m<sup>-2</sup> day<sup>-1</sup>). This shows that the use of these two different approaches can introduce significant uncertainty in the carbon budget and there needs to be both a standardization of techniques and a consensus as to which conversion approach should be employed. The range of results here makes comparison with other studies difficult. For example, the bacterial carbon production values for two glacial snowpacks in the maritime Antarctic (Signy island) that were deduced using radiolabel incorporation experiments were significantly higher than in this study ( $11 \pm 12$  and  $17 \pm 11$  mg C m<sup>-2</sup> d<sup>-1</sup>), but the difference can to some extent be attributed to the higher bacterial cell abundance at Signy ( $10^3$ – $10^4$  cells mL<sup>-1</sup> as opposed to  $10^1$ – $10^3$  cells mL<sup>-1</sup> in this study). With this being the case, the allometric conversions seem most appropriate.

The tendency for net heterotrophy is not in agreement with studies of glacier surface (e.g., Cook et al., 2020; Tedstone et al., 2017; Williamson et al., 2018, 2020) and low elevation snowpacks, such as those in the maritime Antarctic (e.g., Gray et al., 2020). However, it is likely that time, snow cover persistence and nutrient abundance are the key factors differentiating these environments from the system under study. Furthermore, the snowpack at Foxfonna lacked a sufficient autotrophic biomass to start with, with there being virtually none of the so-called snow algae and only modest abundance of cyanobacteria capable of photosynthesis.

## 5. Conclusions

The present study has been one of the first attempts to thoroughly examine a glacial snowpack ecosystem with respect to its seasonal thermal, biogeochemical and microbial community evolution. The mass balance nutrient



data revealed that  $\text{NH}_4^+$  and  $\text{PO}_4^{3-}$ , both essential for biological processes, displayed a non-conservative behavior (as opposed to  $\text{Cl}^-$  and  $\text{NO}_3^-$ ), that is, they did not follow the expected elution dynamics for a melting snowpack. However, this was not due to sequestration by autotrophic communities, but dust fertilization and weathering processes that supplemented the winter atmospheric bulk deposition on the ice cap. Indeed, the average autotrophic abundance on the ice cap throughout the melt season was just  $0.5 \pm 2.7$  cells  $\text{mL}^{-1}$ . Therefore, the total seasonal biological production within the combined layers of snow and SI was dominated by bacteria, allometrically estimated at  $153 \text{ mg C m}^{-2}$ , resulting in a net-heterotrophic (bacterial) snowpack ecosystem.

Superimposed ice formed by the refreezing of percolating meltwater possessed the same chemical and biological features as the overlying snow, and so the percolation of meltwater prior to its formation did not result in any enrichment of nutrients or cells in the ice. For the same reason, biological production within the SI could not be separated from production within the snow. Thus, SI played a passive role, acting as a temporary storage for nutrients and cells and an effective barrier between the snow and the debris- and cell-rich glacier ice that lay beneath.

Bacterial production rates were compared between linear and allometric models of carbon estimation. The latter compared most favorably with studies from the maritime Antarctic and lay in the range  $1.2 \pm 2$ – $1.9 \pm 3.2 \text{ mg C m}^{-2} \text{ day}^{-1}$ . However, since autotrophic cells are so much larger than bacterial cells, carbon budgets will be greatly influenced by summers when snow algae are more successful. On the other hand, since glacial snowpacks will disappear sooner in a warming climate, they are perhaps more likely to be largely net-heterotrophic bacterial ecosystems than autotrophic ecosystems. This is important because fewer nutrients will be assimilated within the snow under these circumstances, and so more will be exported to downstream aquatic ecosystems during early summer.

## Data Availability Statement

The wind-rose diagram presented in Figure S5 from Supporting Information S1 is based on meteorological data collected from the Breinosa weather station, situated near Foxfonna, Svalbard. The data encompasses the study period from 1 April 2016, to 15 August 2016. The raw meteorological data is publicly accessible and can be downloaded from the University Centre in Svalbard (UNIS) website under their weather stations facility section. The data is available at the following URL: <https://www.unis.no/facilities/weather-stations/>.

## Acknowledgments

The authors thank the Commonwealth Scholarship Commission (CSC) for funding through a CSC PhD Scholarship (INCS-2015-214) and the Research Council of Norway BIOICE project (Grant 288402). We thank the University Centre in Svalbard (UNIS) students and logistics team for their help and support during field work. Imaging work was performed at the Wolfson Light Microscopy Facility (LMF), University of Sheffield under the guidance of Dr. Darren Robinson. Dr. Chris Williamson at the University of Bristol is thanked for HPLC analysis on the samples. Wilson (Wai-Yin) Cheung (Queen's University, Canada) is credited for the creation of Figure 1.

## References

- Amato, P., Hennebelle, R., Magand, O., Sancelme, M., Delort, A. M., Barbante, C., et al. (2007). Bacterial characterization of the snow cover at Spitzberg, Svalbard. *FEMS Microbiology Ecology*, *59*(2), 255–264. <https://doi.org/10.1111/j.1574-6941.2006.00198.x>
- Amoroso, A., Domine, F., Esposito, G., Morin, S., Savarino, J., Nardino, M., et al. (2010). Microorganisms in dry polar snow are involved in the exchanges of reactive nitrogen species with the atmosphere. *Environmental Science and Technology*, *44*(2), 714–719. <https://doi.org/10.1021/es9027309>
- Barbesti, S., Citterio, S., Labra, M., Baroni, M. D., Neri, M. G., & Sgorbati, S. (2000). Two and three-color fluorescence flow cytometric analysis of immunoidentified viable bacteria. *Cytometry*, *40*(3), 214–218. [https://doi.org/10.1002/1097-0320\(20000701\)40:3<214::AID-CYTO6>3.0.CO;2-M](https://doi.org/10.1002/1097-0320(20000701)40:3<214::AID-CYTO6>3.0.CO;2-M)
- Bellas, C. M., Anesio, A. M., Telling, J., Stibal, M., Tranter, M., & Davis, S. (2013). Viral impacts on bacterial communities in Arctic cryoconite. *Environmental Research Letters*, *8*(4), 045021. <https://doi.org/10.1088/1748-9326/8/4/045021>
- British Standards Institute. (1996). Water quality—Determination of nitrite nitrogen and nitrate nitrogen and the sum of both by flow analysis (CFA and FIA) and spectrometric detection (pp. 3–17). BS EN ISO 13395.
- British Standards Institute. (2002). Water quality—Determination of soluble silicates by flow analysis (FIA and CFA) and photometric detection (pp. 1–11). BS EN ISO 16254.
- British Standards Institute. (2004). Water quality—Determination of orthophosphate and total phosphorus contents by flow analysis (FIA and CFA)—Part 2: Method by continuous flow analysis (CFA) (Vol. 1-16, p. 153). BS EN ISO 15681.
- British Standards Institute. (2005). Water quality—Determination of ammonium nitrogen—Method by flow analysis (CFA and FIA) and spectrometric detection (pp. 1–18). BS EN ISO 11732.
- Carpenter, E. J., Lin, S., & Capone, D. G. (2000). Bacterial activity in South Pole snow. *Applied and Environmental Microbiology*, *66*(10), 4514–4517. <https://doi.org/10.1128/AEM.66.10.4514-4517.2000>
- Cook, J. M., Hodson, A., Anesio, A., Hanna, E., Yallop, M., Stibal, M., et al. (2012). An improved estimate of microbially mediated carbon fluxes from the Greenland ice sheet. *Journal of Glaciology*, *58*(212), 1098–1108. <https://doi.org/10.3189/2012jog12j001>
- Cook, J. M., Tedstone, A. J., Williamson, C., McCutcheon, J., Hodson, A. J., Dayal, A., et al. (2020). Glacier algae accelerate melt rates on the western Greenland Ice Sheet. *The Cryosphere Discussions*, *14*(1), 1–31. <https://doi.org/10.5194/tc-2019-58>
- Di Mauro, B., Garzonio, R., Baccolo, G., Franzetti, A., Pittino, F., Leoni, B., et al. (2020). Glacier algae foster ice-albedo feedback in the European Alps. *Scientific Reports*, *10*(1), 4739. <https://doi.org/10.1038/s41598-020-61762-0>
- Dubnick, A., Wadham, J., Tranter, M., Sharp, M., Orwin, J., Barker, J., et al. (2017). Trickle or treat: The dynamics of nutrient export from polar glaciers. *Hydrological Processes*, *31*(9), 1776–1789. <https://doi.org/10.1002/hyp.11149>
- Felip, M., Andreatta, S., Sommaruga, R., Straskrbová, V., & Catalan, J. (2007). Suitability of flow cytometry for estimating bacterial biovolume in natural plankton samples: Comparison with microscopy data. *Applied and Environmental Microbiology*, *73*(14), 4508–4514. <https://doi.org/10.1128/AEM.00733-07>

- Felip, M., Sattler, B., Psenner, R., & Catalan, J. (1995). Highly active microbial communities in the ice and snow cover of high mountain lakes, applied and environmental microbiology. Retrieved from <http://aem.asm.org/>
- Fiolka, M. J., Takeuchi, N., Sofińska-Chmiel, W., Wójcik-Mieszawska, S., Irvine-Fynn, T., & Edwards, A. (2021). Morphological and spectroscopic analysis of snow and glacier algae and their parasitic fungi on different glaciers of Svalbard. *Scientific Reports*, *11*(1), 21785. <https://doi.org/10.1038/s41598-021-01211-8>
- Fogg, G. (1967). Observations on the snow algae of the South Orkney Islands. *Philosophical Transactions of the Royal Society of London*, *252*(777), 279–287.
- Fujii, M., Takano, Y., Kojima, H., Hoshino, T., Tanaka, R., & Fukui, M. (2010). Microbial community structure, pigment composition, and nitrogen source of red snow in Antarctica. *Microbial Ecology*, *59*(3), 466–475. <https://doi.org/10.1007/s00248-009-9594-9>
- Gray, A., Krolikowski, M., Fretwell, P., Convey, P., Peck, L. S., Mendelova, M., et al. (2020). Remote sensing reveals Antarctic green snow algae as important terrestrial carbon sink. *Nature Communications*, *11*(1), 2527. <https://doi.org/10.1038/s41467-020-16018-w>
- Grégori, G., Citterio, S., Ghiani, A., Labra, M., Sgorbati, S., Brown, S., & Denis, M. (2001). Resolution of viable and membrane-compromised bacteria in freshwater and marine waters based on analytical flow cytometry and nucleic acid double staining. *Applied and Environmental Microbiology*, *67*(10), 4662–4670. <https://doi.org/10.1128/AEM.67.10.4662-4670.2001>
- Halbach, L., Chevrollier, L. A., Doting, E. L., Cook, J. M., Jensen, M. B., Benning, L. G., et al. (2022). Pigment signatures of algal communities and their implications for glacier surface darkening. *Scientific Reports*, *12*(1), 17643. <https://doi.org/10.1038/s41598-022-22271-4>
- Hamilton, T. L., & Havig, J. (2017). Primary productivity of snow algae communities on stratovolcanoes of the Pacific Northwest. *Geobiology*, *15*(2), 280–295. <https://doi.org/10.1111/gbi.12219>
- Harrold, Z. R., Hausrath, E. M., Garcia, A. H., Murray, A. E., Tschauner, O., Raymond, J. A., et al. (2018). Bioavailability of mineral-bound iron to a snow algal-bacterial coculture and implications for albedo-altering snow algal blooms. In F. E. Löffler (Ed.), *Applied and Environmental Microbiology* (Vol. 84, pp. 1–16). <https://doi.org/10.1128/AEM.02322-17>
- Hell, K., Edwards, A., Zarsky, J., Podmirseg, S. M., Girdwood, S., Pachebat, J. A., et al. (2013). The dynamic bacterial communities of a melting High Arctic glacier snowpack. *The ISME Journal*, *7*(9), 1814–1826. <https://doi.org/10.1038/ismej.2013.51>
- Hinkler, J., Hansen, B. U., Tamstorf, M. P., Sigsgaard, C., & Petersen, D. (2008). Snow and snow-cover in Central Northeast Greenland. *Advances in Ecological Research*, *40*(7), 175–195.
- Hodson, A., Cameron, K., Bøggild, C., Irvine-Fynn, T., Langford, H., Pearce, D., & Banwart, S. (2010a). The structure, biological activity and biogeochemistry of cryoconite aggregates upon an Arctic valley glacier: Longyearbreen, Svalbard. *Journal of Glaciology*, *56*(196), 349–362. <https://doi.org/10.3189/002214310791968403>
- Hodson, A., Nowak, A., Cook, J., Sabacka, M., Wharfe, E. S., Pearce, D. A., et al. (2017). Microbes influence the biogeochemical and optical properties of maritime Antarctic snow. *Journal of Geophysical Research: Biogeosciences*, *122*(6), 1456–1470. <https://doi.org/10.1002/2016JG003694>
- Hodson, A., Roberts, T. J., Engvall, A. C., Holmén, K., & Mumford, P. (2010b). Glacier ecosystem response to episodic nitrogen enrichment in Svalbard, European High Arctic. *Biogeochemistry*, *98*(1–3), 171–184. <https://doi.org/10.1007/s10533-009-9384-y>
- Hodson, A. J., Sabacka, M., Dayal, A., Edwards, A., Cook, J., Convey, P., et al. (2021). Marked seasonal changes in the microbial production, community composition, and biogeochemistry of glacial snowpack ecosystems in the maritime Antarctic. *Journal of Geophysical Research: Biogeosciences*, *126*(7), 1–18. <https://doi.org/10.1029/2020JG005706>
- Hoham, R. W., Berman, J. D., Rogers, H. S., Felio, J. H., Ryba, J. B., & Miller, P. R. (2006). Two new species of green snow algae from Upstate New York. *Chloromonas chenangoensis* sp. nov. and *Chloromonas tughillensis* sp. nov. (Volvocales, Chlorophyceae) and the effects of light on their life cycle development. *Phycologia*, *45*(3), 319–330. <https://doi.org/10.2216/04-103.1>
- Hoham, R. W., & Remias, D. (2020). Snow and glacial algae: A review. *Journal of Phycology*, *56*(2), 264–282. <https://doi.org/10.1111/jpy.12952>
- Hood, E., Battin, T. J., Fellman, J., O'Neel, S., & Spencer, R. G. M. (2015). Storage and release of organic carbon from glaciers and ice sheets. *Nature Geoscience*, *8*(2), 1–6. <https://doi.org/10.1038/ngeo2331>
- Irvine-Fynn, T. D. L., Edwards, A., Newton, S., Langford, H., Rassner, S. M., Telling, J., et al. (2012). Microbial cell budgets of an Arctic glacier surface quantified using flow cytometry. *Environmental Microbiology*, *14*(11), 2998–3012. <https://doi.org/10.1111/j.1462-2920.2012.02876.x>
- Jones, E. L., Hodson, A. J., Thornton, S. F., Redeker, K. R., Rogers, J., Wynn, P. M., et al. (2020). Biogeochemical processes in the active layer and permafrost of a High Arctic Fjord Valley. *Frontiers in Earth Science*, *8*, 1–20. <https://doi.org/10.3389/feart.2020.00342>
- Jones, H. G. (1999). The ecology of snow-covered systems: A brief overview of nutrient cycling and life in the cold. *Hydrological Processes*, *13*(14–15), 2135–2147. [https://doi.org/10.1002/\(sici\)1099-1085\(199910\)13:14<2135::aid-hyp862>3.0.co;2-y](https://doi.org/10.1002/(sici)1099-1085(199910)13:14<2135::aid-hyp862>3.0.co;2-y)
- Kepner, R. L., Wharton, R. A., & Suttle, C. A. (1998). Viruses in Antarctic lakes. *Limnology & Oceanography*, *43*(7), 1754–1761. <https://doi.org/10.4319/lo.1998.43.7.1754>
- Kozioł, K., Katarzyna, K., & Polkowska, Z. (2014). Superimposed ice as a nutrient storage. In *5th international conference on environmental science and technology* (Vol. 69, pp. 139–142).
- Kozioł, K. A. (2014). The provenance, composition and fate of organic carbon on an Arctic Glacier. PhD. thesis. University of Sheffield.
- Kozioł, K. A., Moggridge, H. L., Cook, J. M., & Hodson, A. J. (2019). Organic carbon fluxes of a glacier surface: A case study of Foxfonna, a small Arctic glacier. *Earth Surface Processes and Landforms*, *44*(2), 405–416. <https://doi.org/10.1002/esp.4501>
- Krug, L., Erlacher, A., Markut, K., Berg, G., & Cernava, T. (2020). The microbiome of alpine snow algae shows a specific inter-kingdom connectivity and algae-bacteria interactions with supportive capacities. *The ISME Journal*, *14*(9), 2197–2210. <https://doi.org/10.1038/s41396-020-0677-4>
- Kuhn, M. (2001). The nutrient cycle through snow and ice, a review. *Aquatic Sciences*, *63*(2), 150–167. <https://doi.org/10.1007/p100001348>
- Kühnel, R., Björkman, M. P., Vega, C. P., Hodson, A., Isaksson, E., & Ström, J. (2013). Reactive nitrogen and sulphate wet deposition at Zeppelin Station, Ny-Ålesund, Svalbard. *Polar Research*, *32*(1), 19136. <https://doi.org/10.3402/polar.v32i0.19136>
- Kvíderová, J. (2012). Research on cryosestic communities in Svalbard: The snow algae of temporary snowfields in Petuniabukta, Central Svalbard. *Czech Polar Reports*, *2*(1), 8–19. <https://doi.org/10.5817/cpr2012-1-2>
- Larose, C., Berger, S., Ferrari, C., Navarro, E., Dommergue, A., Schneider, D., & Vogel, T. M. (2010). Microbial sequences retrieved from environmental samples from seasonal Arctic snow and meltwater from Svalbard, Norway. *Extremophiles*, *14*(2), 205–212. <https://doi.org/10.1007/s00792-009-0299-2>
- Larose, C., Dommergue, A., & Vogel, T. (2013). The dynamic Arctic snow pack: An unexplored environment for microbial diversity and activity. *Biology*, *2*(1), 317–330. <https://doi.org/10.3390/biology2010317>
- Lebaron, P., Parthuisot, N., & Catala, P. (1988). Comparison of blue nucleic acid dyes for the flow cytometry enumeration of bacteria in aquatic systems. *Applied and Environmental Microbiology*, *64*(5), 1724–1730.
- Liestøl, O. (1993). In R. S. Williams Jr. & J. G. Ferrigno (Eds.), *Glaciers of Europe—Glaciers of Svalbard, Norway* (pp. E138–E140). U.S. Geological Survey Professional Paper.

- Lutz, S., Anesio, A. M., Raiswell, R., Edwards, A., Newton, R. J., Gill, F., & Benning, L. G. (2016). The biogeography of red snow microbiomes and their role in melting Arctic glaciers. *Nature Communications*, 7(1), 11968. <https://doi.org/10.1038/ncomms11968>
- Malard, L. A., Šabacká, M., Magiopoulos, I., Mowlem, M., Hodson, A., Tranter, M., et al. (2019). Spatial variability of Antarctic surface snow bacterial communities. *Frontiers in Microbiology*, 10, 1–12. <https://doi.org/10.3389/fmicb.2019.00461>
- Michaud, L., Lo Giudice, A., Mysara, M., Monsieurs, P., Raffa, C., Leys, N., et al. (2014). Snow surface microbiome on the High Antarctic Plateau (DOME C). *PLoS One*, 9(8), e104505. <https://doi.org/10.1371/journal.pone.0104505>
- Mikucki, J. A., & Priscu, J. C. (2007). Bacterial diversity associated with blood falls, a subglacial outflow from the Taylor Glacier, Antarctica. *Applied and Environmental Microbiology*, 73(12), 4029–4039. <https://doi.org/10.1128/AEM.01396-06>
- Möller, M., & Möller, R. (2019). *Snow cover variability across glaciers in Nordenskiöldland (Svalbard) from point measurements in 2014–2016* (pp. 1–16). Earth System Science Data Discussions. <https://doi.org/10.1594/PANGAEA.896581>
- Norland, S. (1993). The relationship between biomass and volume of bacteria. In P. F. Kemp, B. F. Sherr, E. B. Sherr, & J. J. Cole (Eds.), *Handbook of methods in aquatic microbiology* (pp. 303–308). Lewis Publishers. Retrieved from <https://www.taylorfrancis.com/books/doi/10.1201/9780203752746/handbook-methods-aquatic-microbial-ecology-paul-kemp-barry-sherr-evelyn-sherr-jonathan-cole>
- Nowak, A., Hodson, A., & Turchyn, A. V. (2018). Spatial and temporal dynamics of dissolved organic carbon, chlorophyll, nutrients, and trace metals in maritime Antarctic snow and snowmelt. *Frontiers in Earth Science*, 6, 201. <https://doi.org/10.3389/feart.2018.00201>
- Onuma, Y., Yoshimura, K., & Takeuchi, N. (2022). *Global simulation of snow algal blooming by coupling a land surface and newly developed snow algae models journal of geophysical research: Biogeosciences*. (Vol. 127). John Wiley and Sons Inc. <https://doi.org/10.1029/2021JG006339>
- Posch, T., Loferer-Kröbächer, M., Gao, G., Alfreider, A., Pernthaler, J., & Psenner, R. (2001). Precision of bacterioplankton biomass determination: A comparison of two fluorescent dyes, and of allometric and linear volume-to-carbon conversion factors. *Aquatic Microbial Ecology*, 25(1), 55–63. <https://doi.org/10.3354/ame025055>
- Priscu, J. C., Tulaczyk, S., Studinger, M., Kennicutt, M. C., Christner, B. C., & Foreman, C. M. (2008). Antarctic subglacial water: Origin, evolution, and ecology. In W. F. Vincent & J. Laybourn-Parry (Eds.), *Polar lakes and rivers: Limnology of Arctic and Antarctic aquatic ecosystems* (pp. 119–135). Oxford University Press.
- Reijmer, C. H., van den Broeke, M. R., Fettweis, X., Ettema, J., & Stap, L. B. (2012). Refreezing on the Greenland ice sheet: A comparison of parameterizations. *The Cryosphere*, 6(4), 743–762. <https://doi.org/10.5194/tc-6-743-2012>
- Remias, D., Schwaiger, S., Aigner, S., Leya, T., Stuppner, H., & Lütz, C. (2012). Characterization of an UV- and VIS-absorbing, purpurogallin-derived secondary pigment new to algae and highly abundant in *Mesotaenium berggrenii* (Zygnematophyceae, Chlorophyta), an extremophyte living on glaciers. *FEMS Microbiology Ecology*, 79(3), 638–648. <https://doi.org/10.1111/j.1574-6941.2011.01245.x>
- Rutter, N., Hodson, A., Irvine-Fynn, T., & Solås, M. K. (2011). Hydrology and hydrochemistry of a deglaciating high-Arctic catchment, Svalbard. *Journal of Hydrology*, 410(1–2), 39–50. <https://doi.org/10.1016/j.jhydrol.2011.09.001>
- Skidmore, M. L., Foght, J. M., & Sharp, M. J. (2000). Microbial life beneath a high Arctic glacier. *Applied and Environmental Microbiology*, 66(8), 3214–3220. <https://doi.org/10.1128/AEM.66.8.3214-3220.2000>
- Stibal, M., Bradley, J. A., & Box, J. E. (2017). Ecological modeling of the supraglacial ecosystem: A process-based perspective. *Frontiers in Earth Science*, 5, 52. <https://doi.org/10.3389/feart.2017.00052>
- Stibal, M., Elster, J., Šabacká, M., & Kaštovská, K. (2007). Seasonal and diel changes in photosynthetic activity of the snow alga *Chlamydomonas nivalis* (Chlorophyceae) from Svalbard determined by pulse amplitude modulation fluorometry. *FEMS Microbiology Ecology*, 59(2), 265–273. <https://doi.org/10.1111/j.1574-6941.2006.00264.x>
- Stibal, M., Gözdereliler, E., Cameron, K. A., Box, J. E., Stevens, I. T., Gokul, J. K., et al. (2015). Microbial abundance in surface ice on the Greenland Ice Sheet. *Frontiers in Microbiology*, 6, 225. <https://doi.org/10.3389/fmicb.2015.00225>
- Takacs, C. D., & Priscu, J. C. (1998). Bacterioplankton dynamics in the McMurdo Dry Valley lakes, Antarctica: Production and biomass loss over four seasons. *Microbial Ecology*, 36(3), 239–250. <https://doi.org/10.1007/s002489900111>
- Takeuchi, N., Dial, R., Kohshima, S., Segawa, T., & Uetake, J. (2006). Spatial distribution and abundance of red snow algae on the Harding Icefield, Alaska derived from a satellite image. *Geophysical Research Letters*, 33(21), 1–6. <https://doi.org/10.1029/2006GL027819>
- Tedstone, A. J., Bamber, J. L., Cook, J. M., Williamson, C. J., Fettweis, X., Hodson, A. J., & Tranter, M. (2017). Dark ice dynamics of the south-west Greenland Ice Sheet. *The Cryosphere*, 11(6), 2491–2506. <https://doi.org/10.5194/tc-11-2491-2017>
- Tranter, M., & Jones, H. G. (2001). The chemistry of snow: Processes and nutrient cycling. *Snow Ecology: An Interdisciplinary Examination of Snow-Covered Ecosystems*, 22(6), 127–167.
- Vimercati, L., Solon, A. J., Krínský, A., Arán, P., Porazinska, D. L., Darcy, J. L., et al. (2019). Nieves penitentes are a new habitat for snow algae in one of the most extreme high-elevation environments on Earth. *Arctic Antarctic and Alpine Research*, 51(1), 190–200. <https://doi.org/10.1080/15230430.2019.1618115>
- Wadham, J. L., De'ath, R., Monteiro, F. M., Tranter, M., Ridgwell, A., Raiswell, R., & Tulaczyk, S. (2013). The potential role of the Antarctic Ice Sheet in global biogeochemical cycles. *Earth and Environmental Science Transactions of the Royal Society of Edinburgh*, 104(1), 55–67. <https://doi.org/10.1017/s1755691013000108>
- Wadham, J. L., Hawkins, J. R., Tarasov, L., Gregoire, L. J., Spencer, R. G. M., Gutjahr, M., et al. (2019). Ice sheets matter for the global carbon cycle. *Nature Communications*, 10(1), 3567. <https://doi.org/10.1038/s41467-019-11394-4>
- Wadham, J. L., & Nuttall, A.-M. (2002). Multiphase formation of superimposed ice during a mass-balance year at a maritime high-Arctic glacier. *Journal of Glaciology*, 48(163), 545–551.
- Whitman, W. B., Coleman, D. C., & Wiebe, W. J. (1998). Prokaryotes: The unseen majority. *Proceedings of the National Academy of Sciences of the United States of America*, 95(12), 6578–6583. <https://doi.org/10.1073/pnas.95.12.6578>
- Williamson, C. J., Anesio, A. M., Cook, J. M., Tedstone, A. J., Poniecka, E., Holland, A., et al. (2018). Ice algal bloom development on the surface of the Greenland Ice Sheet. In *FEMS microbiology ecology* (Vol. 94). Oxford University Press. <https://doi.org/10.1093/femsec/fiy025>
- Williamson, C. J., Cameron, K. A., Cook, J. M., Zarsky, J. D., Stibal, M., & Edwards, A. (2019). Glacier algae: A dark past and a darker future. *Frontiers in Microbiology*, 10, 524. <https://doi.org/10.3389/fmicb.2019.00524>
- Williamson, C. J., Cook, J., Tedstone, A., Yallop, M., McCutcheon, J., Poniecka, E., et al. (2020). Algal photophysiology drives darkening and melt of the Greenland Ice Sheet. *Proceedings of the National Academy of Sciences of the United States of America*, 117(11), 1–12. <https://doi.org/10.1073/pnas.1918412117>
- Wright, A. P., Wadham, J. L., Siegert, M. J., Luckman, A., Kohler, J., & Nuttall, A. M. (2007). Modeling the refreezing of meltwater as superimposed ice on a high Arctic glacier: A comparison of approaches. *Journal of Geophysical Research*, 112(4), 1–14. <https://doi.org/10.1029/2007JF000818>